Experimental evaluation of isentropic efficiency in turbocharger twin-entry turbines

Experimental evaluation of isentropic efficiency in turbocharger twin-entry turbines

Vittorio Usai, Carla Cordalonga, Silvia Marelli

Università degli Studi di Genova

vittorio.usai@edu.unige.it

Abstract. Turbocharging plays a fundamental role not only in improving the performance of automotive engines, but also in reducing the fuel consumption and exhaust emissions of spark-ignited biofuel, diesel, liquid, and gaseous engines. Dedicated experimental investigations on turbochargers are therefore needed to evaluate a better understanding of its performance. The availability of experimental information on the steady flow performance of the turbocharger is an essential requirement to optimize the matching calculation. It is interesting to know the isentropic efficiency of the turbine in order to improve the coupling with the engine, in particular it is difficult to identify the definition of the turbine efficiency through a direct evaluation. In a radial turbine, the isentropic efficiency, evaluated directly starting from the measurement of the thermodynamic quantities at the inlet and outlet sections, can be affected by significant errors. This inaccuracy is mainly related to the incorrect evaluation of the turbine outlet temperature, due to the non-uniform distribution of the flow field in the measurement section. For this purpose, a flow conditioner was installed downstream the turbine. Tests were performed at different values of the rotational speed, and in quasi-adiabatic conditions. The flow field downstream the de-coupler was analysed through a hand-made three-hole probe with an exposed junction thermocouple inserted in the pipe with different protrusions. Thanks to this experimental campaign, it was possible to measure pressure, velocity, mass flow and temperature profiles necessary to examine the homogeneity of the flow field. As the turbocharger is fitted with a twin entry turbine, the thermodynamic quantities have been properly taken into account referring to each sector.

Nomenclature

Definitions

c_p	specific heat at constant pressure

Notations

α	yaw angle
β	compression ratio
ε	expansion ratio
η	efficiency
A	area
c	flow velocity
k	specific heat ratio
M	mass flow rate
n	rotational speed
p	pressure
P	power
T	temperature

Subscripts

1	compressor inlet
2	compressor outlet
3	turbine inlet
31	turbine inlet sector 1
32	turbine inlet sector 2
4	turbine outlet

b	bearings
c	compressor
EXP	experimental
is	isentropic
loc	local
m	mechanical
oil	lubricant oil
S	static condition
t	turbine
T	stagnation condition
TC	turbocharger
w	windage
x	axial
θ	tangential

Acronyms

MFP	Mass Flow Parameter
OEM	Original Equipment Manufacturer
RMS	Root Mean Square

1. Introduction

The regulation imposed by the legislator on the CO_2 emission strongly impact the automotive sector [1]. The OEMs (Original Equipment Manufacturers) are working in order to reduce the pollutant emission; the main strategy, in a short term, is provided by the engine hybridization [2]. In this scenario the performance of the internal combustion engine is still fundamental to reach the required target in terms of both emission and drivability [3]. In order to have more sustainable engines and reduce the dependence on fossil fuel, thus the CO_2 production, an important solution can be provided by bio-fuels [4] and synthetic fuels [5]. To obtain high engine performance, turbocharging still play an important role: specific investigations on turbocharger are fundamental to improve engine-turbocharger 1D models correctly evaluating turbine and compressor behavior [6,7]. The main issue related to the compressor characterization is related to the accurate definition of the characteristic curves taking into account pulsating flow [8], the impact of heat transfer effect at low rotational speed [9] and the position of the surge line [10]. On the turbine side, usually the characteristic curves are defined over a restricted range in steady flow, with the regulation system kept in closed position. Important improvement in the definition of turbine performance can be provided keeping into account the impact of the pulsating flow [11] and different position of the regulating system [12]. Moreover, multy-entry turbine should be characterized over an extended range of admission condition, and not only in full admission. The adoption of twin entry turbines, with a proper design of the exhaust circuit, can allow significant improvements in fuel consumption and transient response [13]. In order to correctly evaluate twin entry turbine performance, specific parameters have to be considered. In following equations parameters are described according to the Reynolds and Mach similarity theory that guarantee comparison between the turbocharger performance in different test conditions.

The Turbine Speed Parameter is defined as:

$$N_t = \frac{n_{TC}}{\sqrt{T_{T3}}} \qquad \left[\frac{rpm}{\sqrt{K}}\right] \quad (1)$$

Due to the twin-entry configuration, T_{T3} is calculated as the air mass flow rate mean of the total temperature:

$$T_{T3} = \frac{M_{t31} \cdot T_{T31} + M_{t32} \cdot T_{T32}}{M_{t31} + M_{t32}} \qquad [K] \quad (2)$$

The Expansion Ratio of the turbine (total-to-static) is reported in equation 3:

$$\varepsilon_{tTS} = \frac{p_{T3}}{p_{s4}} \quad [-] \quad (3)$$

In full and unequal admission p_{T3} is defined as the area mean of total pressure of each sector:

$$p_{T3} = \frac{p_{T31} \cdot A_{31} + p_{T32} \cdot A_{32}}{A_{31} + A_{32}} \quad [bar] \quad (4)$$

The Mass Flow Parameter has to be defined over each sector as showed in equations 5 and 6:

$$MFP_1 = \frac{M_{t31} \cdot \sqrt{T_{T31}}}{p_{T31}} \quad \left[\frac{kg\sqrt{K}}{s\ bar}\right] \quad (5)$$

$$MFP_2 = \frac{M_{t32} \cdot \sqrt{T_{T32}}}{p_{T32}} \quad \left[\frac{kg\sqrt{K}}{s\ bar}\right] \quad (6)$$

The overall Mass Flow Parameter is defined as:

$$MFP = \frac{M_{t3} \cdot \sqrt{T_{T3}}}{p_{T3}} \quad \left[\frac{kg\sqrt{K}}{s\ bar}\right] \quad (7)$$

where M_{t3} is the total air mass flow rate calculated as the sum of the mass flow rate in the two sectors, while T_{T3} and p_{T3} are defined according with the equations (2) and (4).
Another important issue of the turbine characterization is provided by the correct evaluation of the efficiency. Using the turbocharger testing procedure according to SAE guidelines [14] the direct evaluation of the isentropic efficiency is not possible with a high degree of accuracy. For this reason, it is frequent practice to refer to the thermomechanical efficiency:

$$\eta_t{}' = \eta_{tTS} \cdot \eta_m = \frac{P_t}{P_{t\,is}} \cdot \frac{P_c}{P_t} = \frac{P_c}{P_{t\,is}} = \frac{M_c c_{pc} (T_{T2} - T_{T1})}{M_t c_{pt} T_{T3} \left[1 - \left(\frac{p_{S4}}{p_{T3}}\right)^{\frac{k-1}{k}}\right]} \quad [-] \quad (8)$$

This choice is given by the strong non-uniformity of the turbine outlet temperature field [15], which makes it difficult to correctly measure the isentropic efficiency, defined as:

$$\eta_{tTS} = \frac{T_{T3} - T_{T4}}{T_{T3} - T_{S4is}} = \frac{T_{T3} - T_{T4}}{T_{T3} \left[1 - \left(\frac{p_{S4}}{p_{T3}}\right)^{\frac{k-1}{k}}\right]} \quad [-] \quad (9)$$

The correct evaluation of the turbine isentropic efficiency allow important improvements in the 1D models on the matching between turbocharger, engine and after-treatment system.
In order to overcome the issue related to the correct measurement of the turbine outlet temperature, the most common solution to evaluate the turbine isentropic efficiency is provided by an indirect evaluation starting from equation 8. This approach requires the assessment of the mechanical efficiency η_m that can be defined as:

$$\eta_m = \frac{P_c}{P_t} = \frac{P_c}{P_c + P_b + P_w} \quad [-] \quad (10)$$

The power dissipated in the bearings (P_b) can be evaluated as heat flow transferred to the lubricating oil [16]:

$$P_b = M_{oil} c_{p,oil} \left(T_{oil,out} - T_{oil,in}\right) \quad [-] \quad (11)$$

The windage losses (P_w), on the other hand, can be evaluated through semiempirical correlations, as proposed in [17].
The literature is so poor about the possibility to directly evaluate the turbine isentropic efficiency; Biet et al. [18,19] proposed a solution to obtain a direct evaluation of the turbine isentropic efficiency using a mixing device in the pipe downstream the turbine. Experimental tests under quasi-adiabatic condition are performed to compare the experimental tests with the results of a CFD model in adiabatic condition. With the employed setup, a direct and unhindered way to investigate the aerodynamic properties has been found. Moreover, the comparison with the numerical investigations shows that the results obtained are plausible.
In this work, different turbine outlet measuring stations are presented to obtain a good evaluation of the isentropic efficiency for a twin entry turbocharger usually equipped on 10 liters heavy duty diesel engine. To this aim, 3 different turbine outlet measuring station layout are presented in order to find the best solution in terms of temperature uniformities without compromising the evaluation of the swallowing capacity curves. Moreover, a slightly intrusive 3-hole probe with exposed junction thermocouple was adopted to perform local measurement of the flow and temperature field at the turbine outlet. Therefore, since the flow is regularized showing the absence of swirl components, it was possible to evaluate efficiency through the standard temperature measuring station. Results obtained through the not-standard measuring station are compared with those achieved through a direct measurement of turbine outlet temperature by three probes inserted in the pipe without the flow conditioning device. Even if the temperature is uniform at the outlet of the turbine thanks to the adoption of the flow conditioning device, it seems that the heat transfer effect across the pipes and across the turbocharger components still plays an important role on the estimation of the temperature at the outlet section. Further step will regard an extension of investigations in a wider range of turbine operating conditions and in quasi-adiabatic conditions. Furthermore, a methodology will be defined to perform a realistic measurement of turbine outlet temperature in a simpler, less time-consuming way, taking into account not only the temperature field but also heat transfer effects.

2. Experimental Set up and Test program

The experimental investigation was carried out at test bench for components of propulsion systems of the University of Genoa (‘figure 1’).

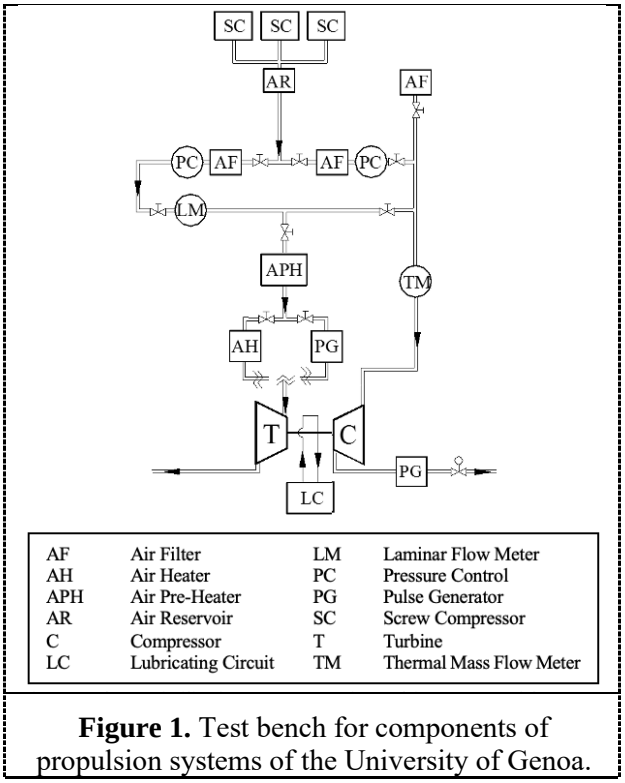

Figure 1. Test bench for components of propulsion systems of the University of Genoa.

Three screw compressors, operating in parallel, deliver a total mass flow rate of 0.65 kg/s at a maximum pressure of 8 bar.

"Cold" and "Hot" tests can be performed thanks to electric heaters, with maximum operating temperature of 750°C.

LabVIEW® is used as data acquisition and processing system through interactive procedures.

Several average parameters are measured upstream and downstream compressor and turbine. Static pressures are measured using strain-gauge and piezoresistive transducers (accuracy of ±0.15% of full scale). Platinum resistance thermometers (with an accuracy of ±0.15 ◦C ± 0.2% of measured value) and thermocouples are used to measure total temperatures. Compressor mass flow rate is measured with a thermal mass flow meter (with an accuracy of ±0.9% measured value and ±0.05% of the full scale). Turbine mass flow rate is measured through a laminar flow meter (with an accuracy of ±2% of the measured value). Turbocharger rotational speed is captured using an eddy current probe (with an accuracy of ±0.009% of the measured value).

To properly control and regulate the air mass flow rate at each turbine inlet, two throttle valves are installed for each sector. These can be controlled through a voltage signal from the completely closed to the fully open position. In order to measure the mass flow rate in each sector of the turbine, a flange with a calibrated orifice is installed. The hole diameter is dimensioned by the manufacturer to generate a specific pressure difference measured by two dedicated differential pressure transducers. The experimental set-up above described is shown in 'figure 2'.

Figure 2. Turbine feeding line and flange with a calibrated orifice.

The experimental investigation was performed on a turbocharger for heavy duty application (compressor impeller diameter 78.5 mm, and turbine rotor diameter 69.5 mm).
In ‘figure 3’ the characteristic curves of the turbine are presented for 5 different turbine rotational speed factor levels in full and partial admission. The two sectors are characterized by a different swallowing capacity, with the sector 2 (shroud side) characterized by a higher swallowing capacity than sector 1 (hub side). Moreover, it is possible to note that the mass flow rate parameter in full admission cannot be calculated as the sum of the mass flow parameters of each sector. A more detailed analysis on the behaviour of the turbine in different admission conditions is reported in [20].

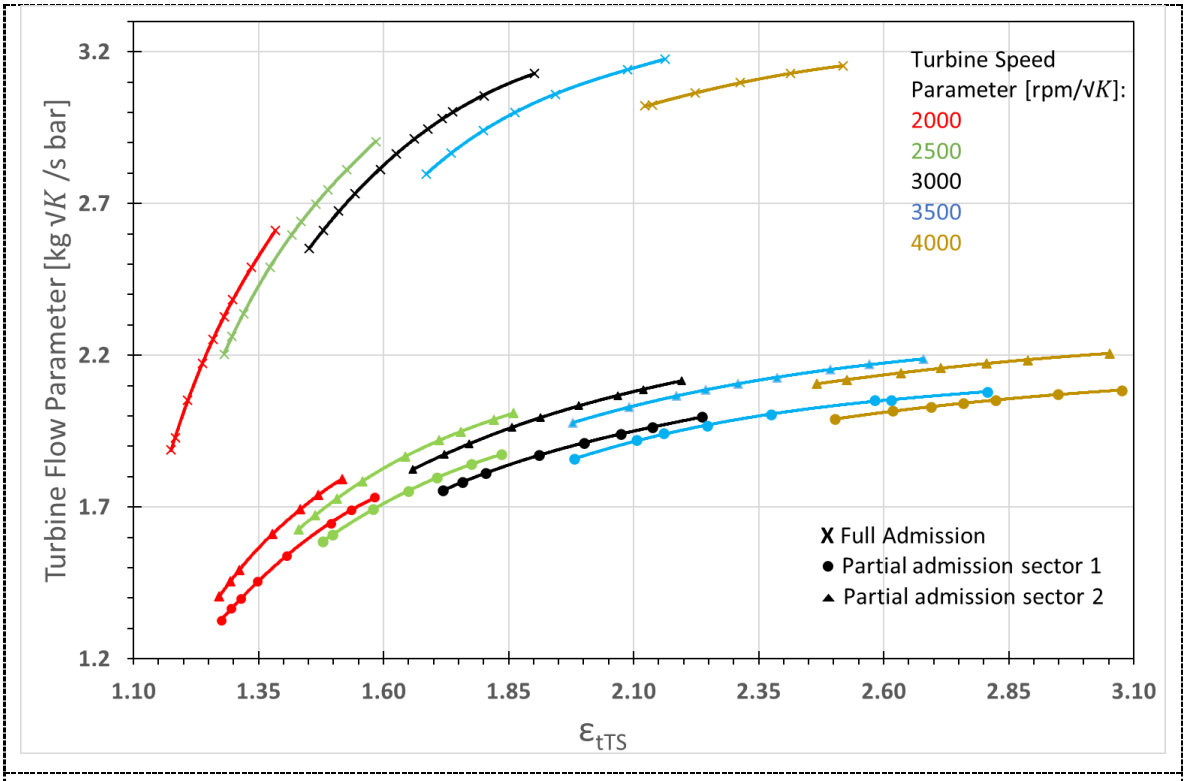

Figure 3. Turbine swallowing capacity curves

During the test campaign, three different configurations at the turbine outlet line ('figure 4') were tested, in the presence and without the flow conditioning device, considering different positions of the pressure measuring stations. The configuration 1 is the standard measuring station without the flow conditioning device, the configuration 2 is characterized by the presence of the flow conditioning device, the configuration 3 refers to the adoption of the flow conditioning device with the pressure measuring station placed between the turbine and the flow conditioner.

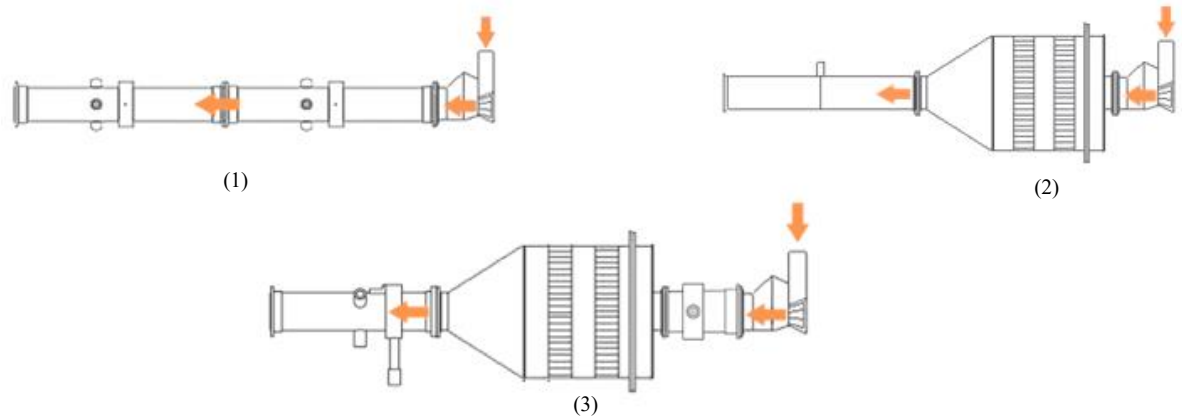

Figure 4. Different turbine outlet configurations at the turbine outlet.

In 'figures 5 and 6' a comparison between the characteristic curves of the turbine using different configurations is reported. Results obtained using configuration 2 (blue line) highlight that the pressure losses generated by the flow conditioning device, especially at higher rotational speeds, are not negligible and introduce not-acceptable differences with respect to the reference condition (configuration 1, red line) due to the high level of mass flow rate.

For this reason, in configuration 3 the pressure measuring station was moved closed to the turbine outlet in order to allow a proper evaluation of the turbine outlet pressure avoiding pressure losses across the flow conditioning device. This aspect is confirmed by the green lines (configuration 3) quite perfectly overlapped to the red lines.

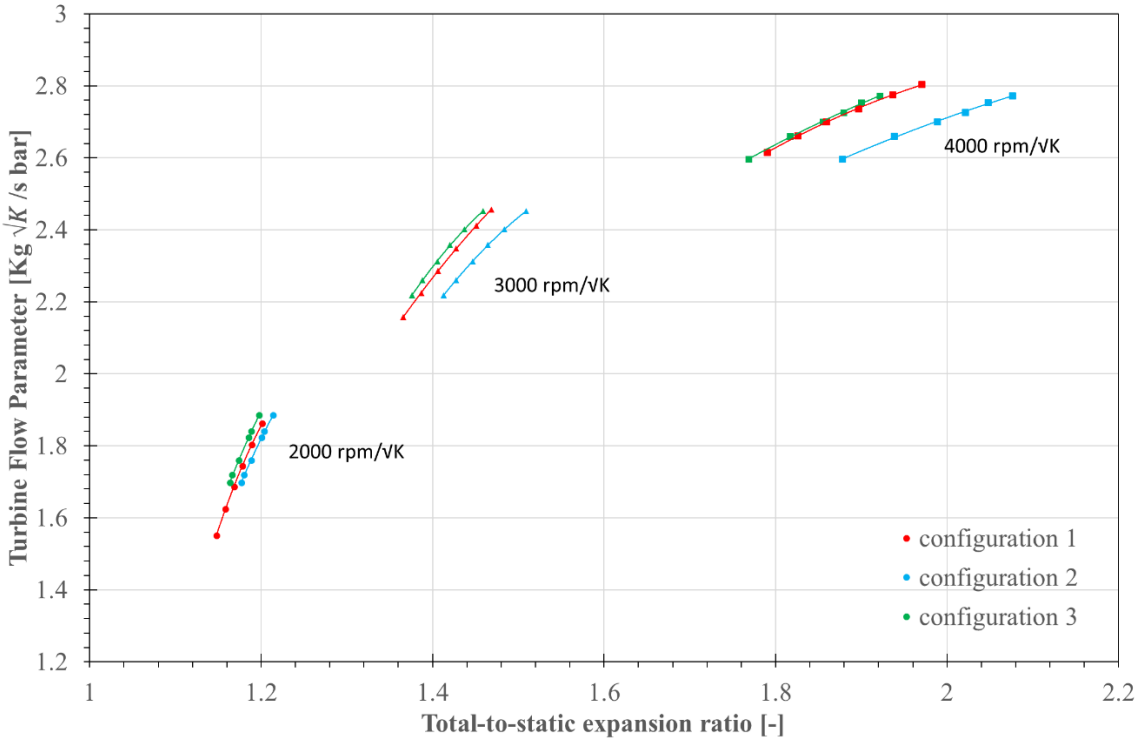

Figure 5. Comparison of the turbine swallowing capacity in different layout configurations.

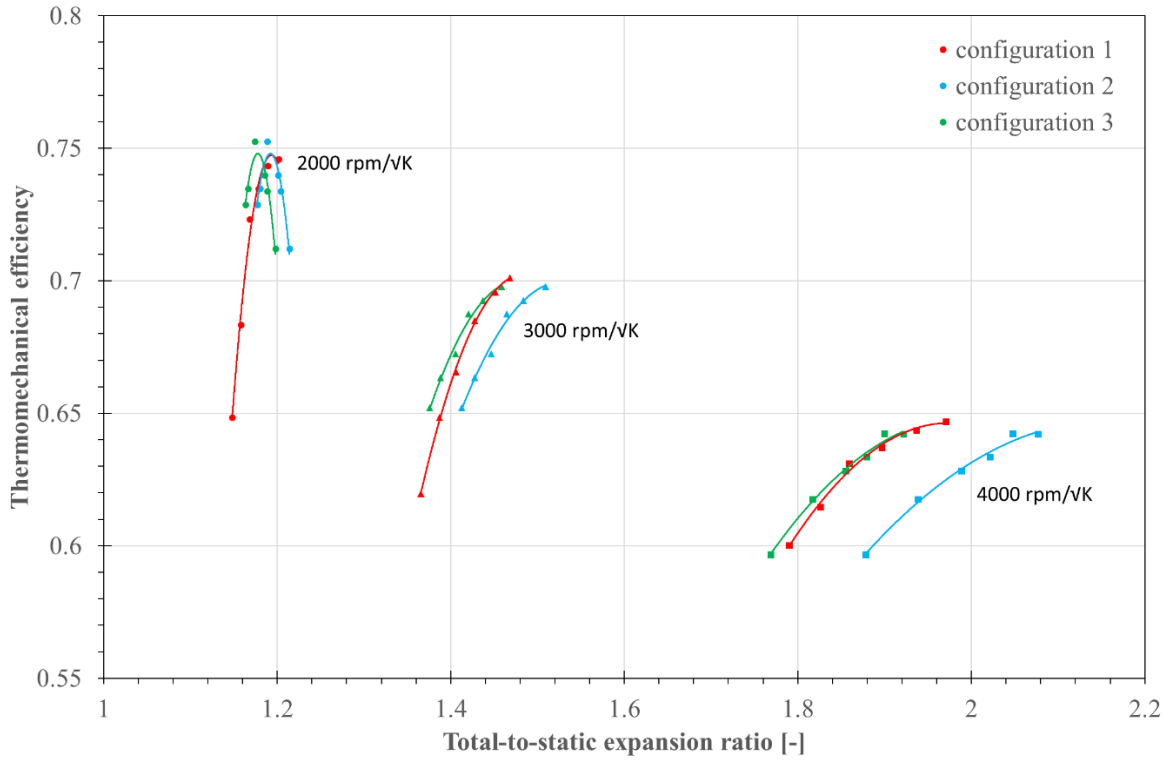

Figure 6. Comparison of the turbine thermomechanical efficiency in different layout configurations.

The flow conditioner presents an abrupt section widening in the flow direction from 50mm to 200mm, allowing the installation of internal elements. Based on previous studies developed using different elements [21,22], two honeycombs placed in series are adopted to dissipates the flow structures dominated by vorticity, achieving a uniform distribution of the velocity and temperature fields. The effect of the flow conditioning device is highlighted by the variation of the RMS value of the temperature measured downstream the flow conditioner using the standard measuring station through the three thermocouples crosswise inserted in the pipe. In ‘figure 7’, a comparison between the configuration 1 and 3 is shown. The reduction of RMS values in configuration 3 demonstrates a decrease of the non-uniform distribution of the temperature field.

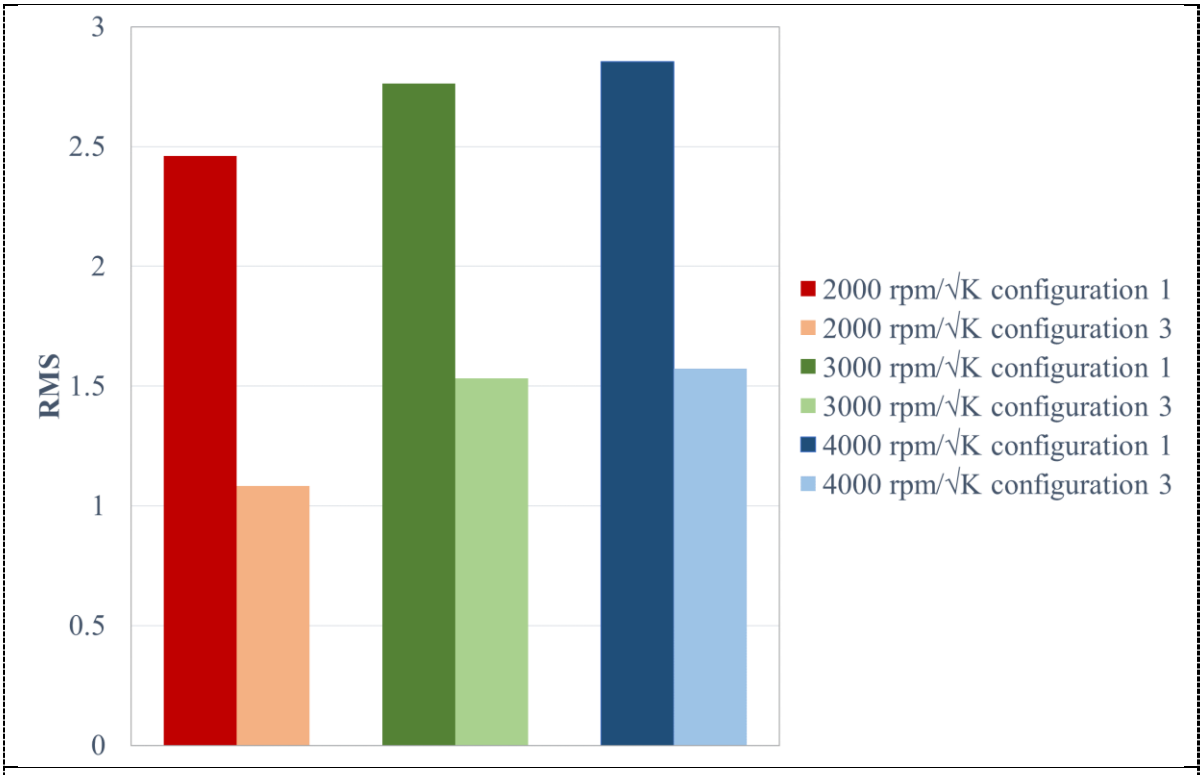

Figure 7. Comparison of the RMS of temperature with and without the flow conditioning device.

The purpose of the flow conditioning device is the direct evaluation of the isentropic efficiency of the turbine adopting the downstream standard temperature measuring station characterized by three thermocouples. Passing through the flow conditioner, flow tangential velocity is reduced almost to zero. To validate the configuration 3, a hand-made slight intrusive three-hole probe equipped with an exposed junction thermocouple ('figure 8 in the right') has been used to investigate the flow and the temperature distribution.

The three-hole probe was calibrated using a specific calibrated nozzle, as shown in 'figure 8 on the left'.

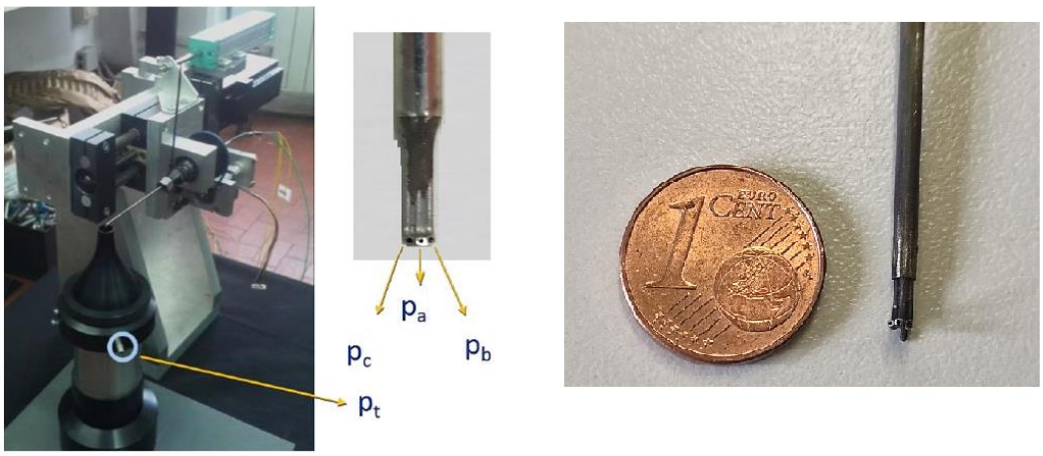

Figure 8. Three-hole probe calibration system (left) and a detail of the three-hole probe with exposed junction thermocouple (right).

This calibration method employs the definition of the calibration coefficients of the probe [23]; by varying the angle of rotation, the calibration curves are thus obtained (‘figure 9’).

$$C_{p_T} = \frac{p_a - p_T}{p_T - p_S} \tag{12}$$

$$C_b = \frac{p_c - p_b}{p_T - p_S} = \frac{\Delta p_{cb}}{p_T - p_S} \tag{13}$$

$$C_{p_S} = \frac{\frac{p_b + p_c}{2} - p_S}{p_T - p_S} \tag{14}$$

where a, b and c correspond to the holes of the probe as shown in ‘figure 8’.

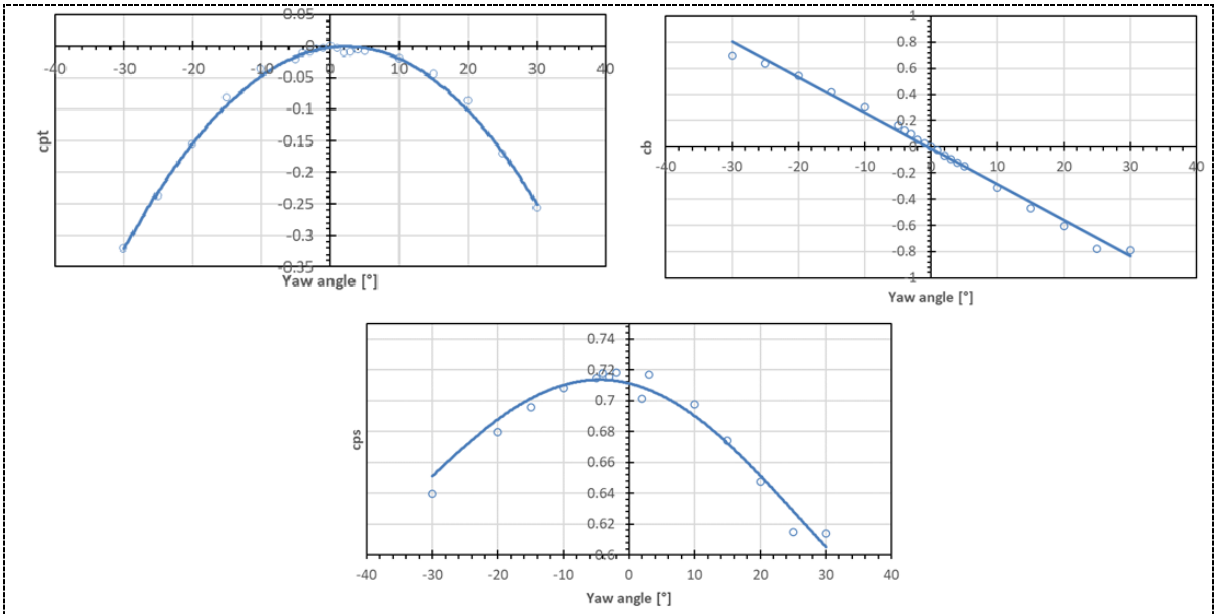

Figure 9. Three-hole probe calibration curves C_{p_T}, C_b, C_{p_S}.

Starting from the calibration curves, it is possible to obtain, through an iterative cycle, the information about the axial velocity, the tangential velocity c_θ, local temperature and pressure.
The investigation was carried out considering a matrix of 9 radial positions at the flow conditioner outlet, not equally spaced to avoid a not realistic local mass flow profile (‘figure 10’) [15].

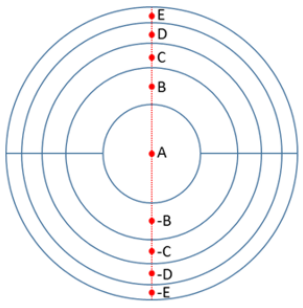

Measuring Point	Radial position [mm]
A	0
B	12.2
C	17.7
D	21.8
E	25

Figure 10. Discretization of the measuring section.

The experimental activity was carried out for three different turbine rotational speed factor ($n/\sqrt{T_{T3}}$) equal to 2000, 3000 and 4000 $rpm/\sqrt{K}$. Moreover, tests were carried out in full admission and in cold condition (with a turbine inlet temperature equal to 80°C); a detailed overview of the operating points analyzed is shown in table 1.

Table 1. Operating Conditions

N_t	T_{T3}	MFP	ε_{tTS}
[rpm/√K]	**[°C]**	**[(kg*√K) / (s*bar)]**	**[-]**
2000	*80*	*1.64*	*1.15*
		1.70	*1.16*
		1.75	*1.17*
		1.84	*1.18*
3000	*80*	*2.21*	*1.37*
		2.26	*1.39*
		2.32	*1.41*
		2.45	*1.45*
4000	*80*	*2.60*	*1.77*
		2.64	*1.80*
		2.70	*1.85*
		2.75	*1.90*

3. Results

Comparing the experimental tangential velocity profiles (‘figure 11’) with an ideal profile, it can observe that the tangential component is not zero in the centre of the duct, probably due to a not perfect alignment of the probe.

Therefore, it was necessary to evaluate the mean yaw angle of the flow from the equation:

$$\bar{\alpha}_0 = \frac{1}{n}\sum_{i=1}^{n} tan^{-1}\left(\frac{C_{\vartheta 0_i}}{C_{x0_i}}\right) \tag{15}$$

where:

i is the i-th probe position;

0 is the radial position in the centre of the pipe;

n is the number of operating conditions.

The tangential velocity profiles corrected on the basis of equation 15 are reported in ‘figure12’ and present a more reliable trend with the ideal ones.

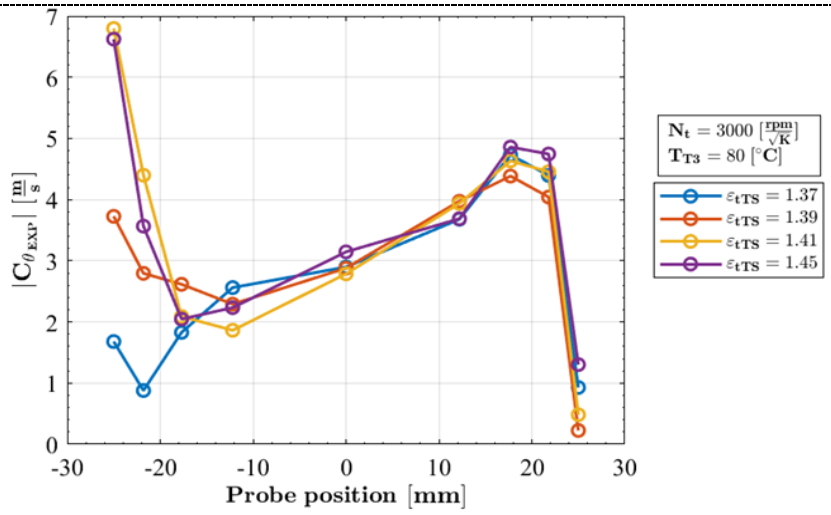

Figure 11. Experimental tangential velocity profiles.

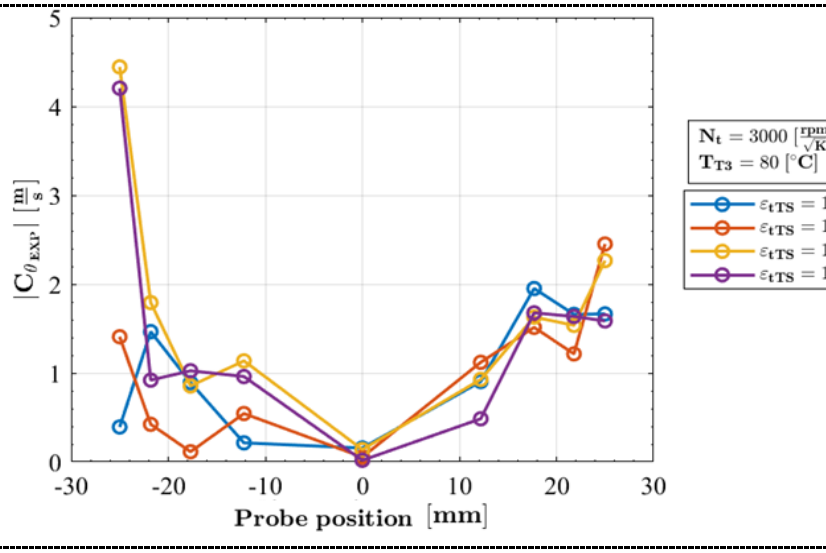

Figure 12. Corrected tangential velocity profiles.

In ‘figure 13’ the axial and the tangential velocity profile are reported on the same plot in order to highlight the effects of the conditioning device on the flow field.

The comparison between the axial and the tangential velocities shows that the flow maintains the same structure in the operating conditions analysed. The values of the tangential components are rather low compared to the axial ones, suggesting no marked swirl component.

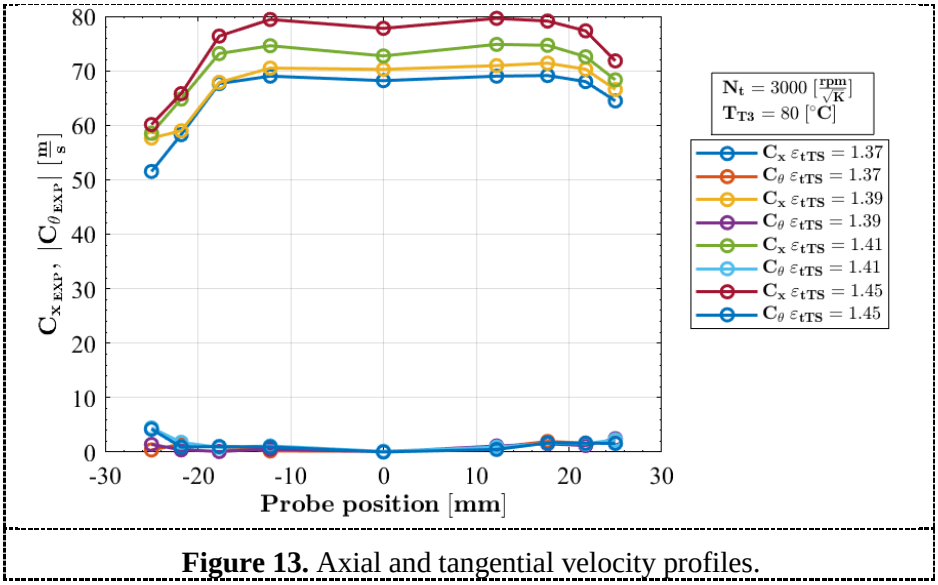

Figure 13. Axial and tangential velocity profiles.

The reduction in tangential velocity is therefore followed by a homogenization of the temperature profiles. As shown in 'figure 14' the temperature field is almost constant along the measuring section.

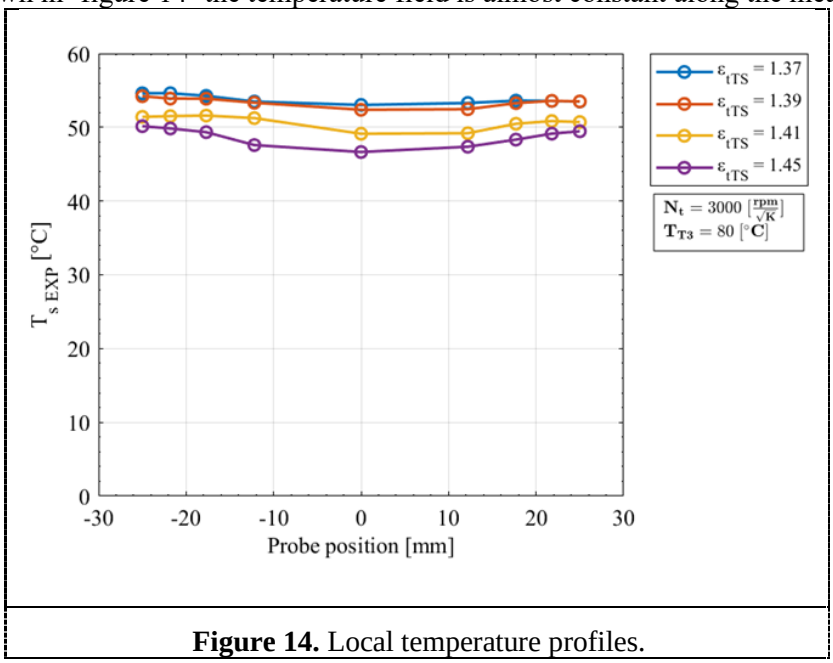

Figure 14. Local temperature profiles.

After evaluating the characteristic of the flow downstream the flow conditioning device, the mass flow profiles are following analyzed. The local mass flow is defined as:

$$M_{loc,i} = \rho_i \cdot c_{x,i} \cdot A \tag{16}$$

where:
i is the i-th probe position;
$M_{loc,i}$ is the local mass flow rate;
A is the local measuring section.
Since the density is almost constant due to the good uniformities of the temperature field, the local mass flow profile results like the axial velocity profile, as shown in 'figure 15'.

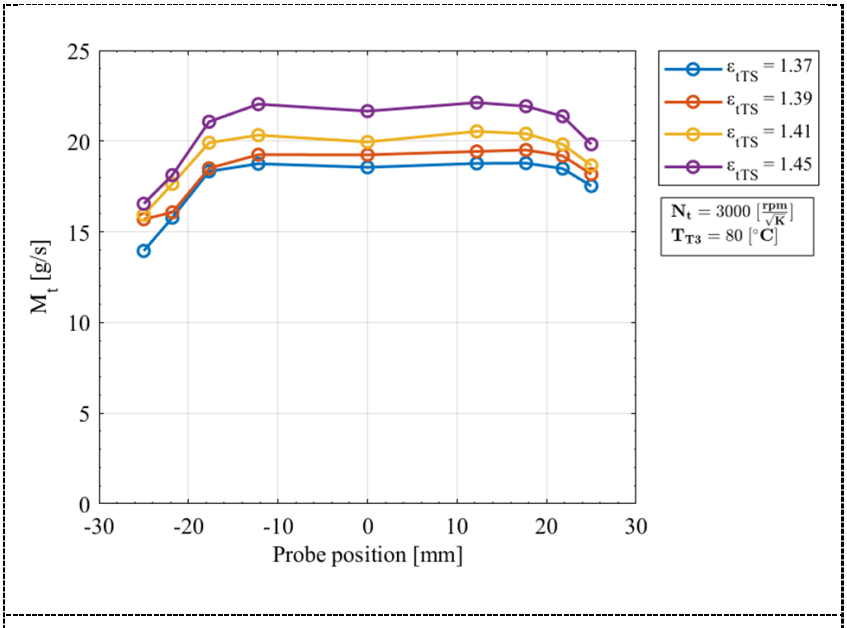

Figure 15. Local mass flow rate profiles.

Results obtained through the use of the three-hole probe highlight a good homogenization of the temperature and velocity field.

Therefore, in 'figure 16' a comparison between the thermomechanical and isentropic efficiencies measured in the presence (respectively in blue and orange lines) and without (respectively in purple and green) the flow conditioning device is reported. As previously stated in 'figure 6', the thermomechanical curves are almost overlapped since the flow conditioning device does not affects this parameter, since this quantity is not affected by the turbine outlet temperature (see equation 8).

As previously demonstrated, the flow conditioning device seems to provide a good uniformity of flow and temperature fields, the direct isentropic efficiency is then calculated adopting the standard temperature measuring station with three thermocouples crosswise inserted in the pipe. The turbine isentropic efficiency measured with the flow conditioner is shown in orange while the efficiency calculated without the flow conditioning device is represented in green. It can be observed that the efficiency directly measured with the device installed presents higher values with respect to the case without the flow conditioner. As a matter of fact, the non-uniform distribution of temperature and flow field, in the condition analyzed in this paper, cause an underestimation of the isentropic efficiency mainly due to the incorrect measurement of the temperature at the turbine outlet because of inhomogeneous flow.

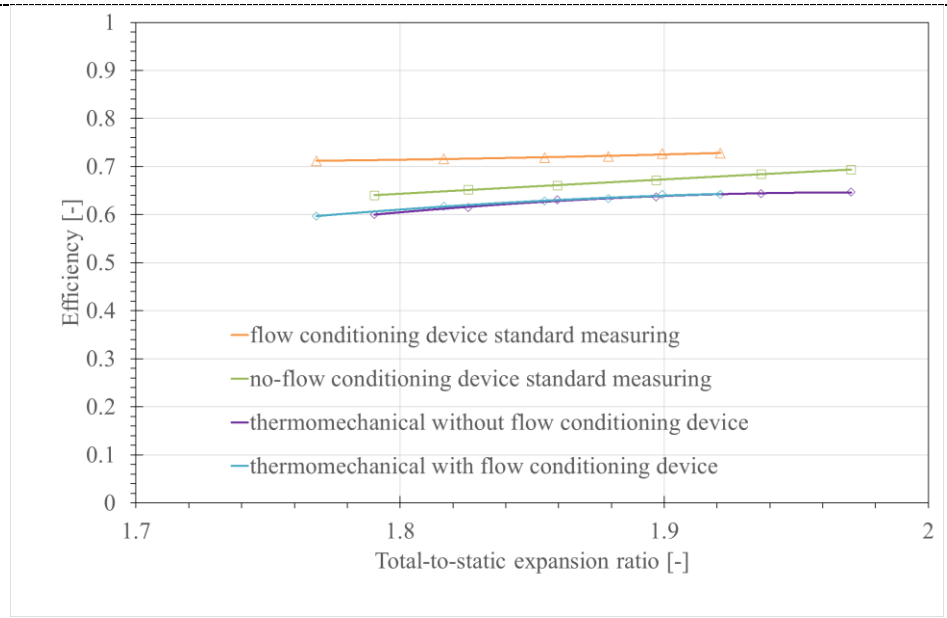

Figure 16. Thermomechanical and isentropic turbine efficiency in configuration 1 and 3.

4. Conclusion

The knowledge of the isentropic efficiency of turbochargers plays a fundamental role in the engine-turbocharger matching calculation. Moreover, the correct assessment of the turbine isentropic efficiency allows a more accurate evaluation of the outlet temperature, which corresponds to the inlet temperature of the aftertreatment system. This information is of high interest, mainly related to the optimisation of the catalyst heating time thus reducing pollutant emissions.

In this paper an experimental method is proposed to directly evaluate the isentropic efficiency of small radial turbines. To this aim, a flow conditioning device is developed, and its behaviour is evaluated through a specific experimental campaign with a slight intrusive three-hole probe with exposed junction thermocouple. Particular attention was paid to the flow and temperature field downstream the flow conditioner to highlight if the flow characteristic is adequate to perform a reliable evaluation of the turbine efficiency through a standard measuring station, thanks to the temperature homogenization.

The results obtained are very encouraging and it seems that a proper evaluation of the efficiency is achieved. Anyway, in further works a wider dataset will be considered taking into account different turbine operating conditions, such as different admission condition, in order to better understand the impact of the flow field at the turbine outlet on the flow conditioning device. Moreover, different turbine inlet temperature will be tested to evaluate the impact of heat transfer effects on the flow conditioner response.

References

[1] Song J., Cha J., "Development of prediction methodology for CO2 emissions and fuel economy of light duty vehicle," Energy, (2022). DOI: 10.1016/j.energy.2022.123166.
[2] Won H.W., Bouet A., "Toward the European 2030 CO2 target with gasoline compression ignition technology and 48 V mild electric hybrid," International Journal of Engine Research, (2022). DOI: 10.1177/14680874221080299.
[3] Marelli S., Usai V., "Experimental analysis and 1D simulation of an advanced hybrid boosting system for automotive applications in transient operation," International Journal of Engine Research, (2021). DOI: 10.1177/14680874211060173.
[4] Zamboni G., Capobianco M., "Definition of the optimal content of used cooking oil methyl ester in blends fuelling a turbocharged diesel engine," Biomass and Bioenergy, (2021). DOI: 10.1016/j.biombioe.2021.106098.
[5] Pöllmann S., Härtl M., Wachtmeister G., "Potential of miller timing with synthetic diesel fuels on a single cylinder heavy-duty engine," International Journal of Engine Research, (2022). DOI: 10.1177/14680874211043649.
[6] Gurney D., "The design of turbocharged engines using 1D simulation,", 2001, SAE Technical Papers 2001-01-0576, (2001). DOI: 10.4271/2001-01-0576.
[7] Piscaglia F., Onorati A., Marelli S., Capobianco M., "A detailed one-dimensional model to predict the unsteady behavior of turbocharger turbines for internal combustion engine applications," International Journal of Engine Research, (2019). DOI: 10.1177/1468087417752525.
[8] Yang M., Shu M., Yang B., Martinez-Bota, R., Deng K. "Unsteady response of performance for centrifugal compressor under pulsating backpressure condition," Aerospace Science and Technology, (2022). DOI: 10.1016/j.ast.2022.107589.
[9] Sirakov B., Casey M., "Evaluation of Heat Transfer Effects on Turbocharger Performance," Journal of Turbomachinery, (2013). DOI: 10.1115/1.4006608.
[10] Marelli S., Silvestri P., Usai V., Capobianco M. "Incipient Surge Detection in Automotive Turbocharger Compressors," SAE Technical Papers, (2019). DOI: 10.4271/2019-24-0186.
[11] Mosca R., Lim S.M., Mihaescu M., "Turbocharger Radial Turbine Response to Pulse Amplitude," Journal of Energy Resources Technology, Transactions of the ASME, (2022). DOI: 10.1115/1.4053346.
[12] Usai V., Marelli, S., Renuke, A., Traverso, A., "Energy Harvesting Technology for turbocompounding automotive engines with waste-gate valve," E3S Web of Conferences, (2019). DOI: 10.1051/e3sconf/201911303020.
[13] Wei J., Xue Y., Deng K., Yang M., Liu Y., "A direct comparison of unsteady influence of turbine with twin-entry and single-entry scroll on performance of internal combustion engine," Energy, (2020). DOI: 10.1016/j.energy.2020.118638.
[14] Society of Automotive Engineers. SAE-Standard J922: Turbocharger nomenclature and terminology. Warrendale, PA: SAE, 1995.
[15] Marelli S., Usai V., Capobianco M., Montenegro G., Della Torre A., Onorati A., "Direct evaluation of turbine isentropic efficiency in turbochargers: Cfd assisted design of an innovative measuring technique," SAE Technical Papers, (2019). DOI: 10.4271/2019-01-0324.
[16] Deligant M., Podevin P., Descombes G., "Experimental identification of turbocharger mechanical friction losses," Energy, (2012). DOI: 10.1016/j.energy.2011.12.049.
[17] Daily J., Nece R., "Chamber dimension effect on induced flow and frictional resistance of enclosed rotating disks," Journal of Fluids Engineering, Transactions of the ASME, (1960). DOI: 10.1115/1.3662532.
[18] Biet C, Boxberger V, Mai H, Zimmermann R., "New evaluation of turbocharger components based on turbine outlet temperature measurements in adiabatic conditions," In: 15th international symposium on transport phenomena and dynamics of rotating machinery, (2014).
[19] Zimmermann R., R Baar B., Biet C.,"Determination of the isentropic turbine efficiency due to adiabatic measurements and the validation of the conditions via a new criterion," Proceedings of the

Institution of Mechanical Engineers, Part C: Journal of Mechanical Engineering Science, (2018). DOI: 10.1177/0954406216670683.
[20] Usai V., Marelli S., "Steady state experimental characterization of a twin entry turbine under different admission conditions," Energies, (2021). DOI: 10.3390/en14082228.
[21] Marelli S., Usai V., Cordalonga C., Capobianco M., "An innovative measurement technique for the direct evaluation of the isentropic efficiency of turbocharger turbines," Proceedings of the ASME Turbo Expo, (2022).
[22] Marelli S., Marmorato G., Capobianco M, Boulanger, JM., "Towards the Direct Evaluation of Turbine Isentropic Efficiency in Turbocharger Testing," SAE Technical Papers, (2016). DOI: 10.4271/2016-01-1033.
[23] Argüelles Díaz K.M., Fernández Oro J.M., Blanco Marigorta E., "Cylindrical three-hole pressure probe calibration for large angular range," Flow Measurement and Instrumentation, (2009). DOI: 10.1016/j.flowmeasinst.2008.12.001.